Barry Industries, Inc.

Finite Element Analysis of a High Power Resistor

prepared by: Barry Industries, Inc.

date: 07 April 1996

Finite Element Analysis of a High Power Termination

Overview

The finite element analysis described in this report was performed to support the conclusions of the Barry Industries' report "Materials Selection for High-Power / High Reliability Resistors", Jack Lackner, May 1995.   The device temperatures and subsequent stresses induced during maximum rated power dissipation are presented.

Simplifying Assumptions

Since the primary objective of the analysis was to obtain the stresses in the bonding layer between the resistor substrate and the carrier, several of the construction details which would not significantly influence this behavior were omitted from the model. The plating layers were not modeled since the thickness of these layers dictate that the thermal expansion of the base materials would not be affected. Including these thin layers would also have introduced modeling elements of drastic aspect ratio. Such elements tend to degrade the analysis accuracy, particularly in stress calculations.

It is further assumed that the convection and radiation effects are negligible, and therefore the majority of the dissipated energy is conducted to the heat sink through the carrier.   This leads to the elimination of the lead structures, glass passivation layer and the cover plate from this analysis. The thermal analysis shows a temperature rise from the bottom of the carrier to the top of the resistive film of less than 50 Celsius degrees.   As long as the device is mounted in a closed box, these assumptions are reasonable.

In addition, since a comparison of the maximum stress condition was the objective, a linear static analysis was performed. While greater detail is obtained in non-linear and or transient type analyses, the linear static type provides an adequate comparison between the two designs.

Model Design

The implementation used is a full three dimensional finite element model which takes advantage of the inherent symmetry of the device in two planes to significantly reduce the computation required for solution. The geometry of the device is shown in Fig. 1. The symmetry chosen has the additional benefit that temperature contours in the critical center planes of the device are readily available without further processing.
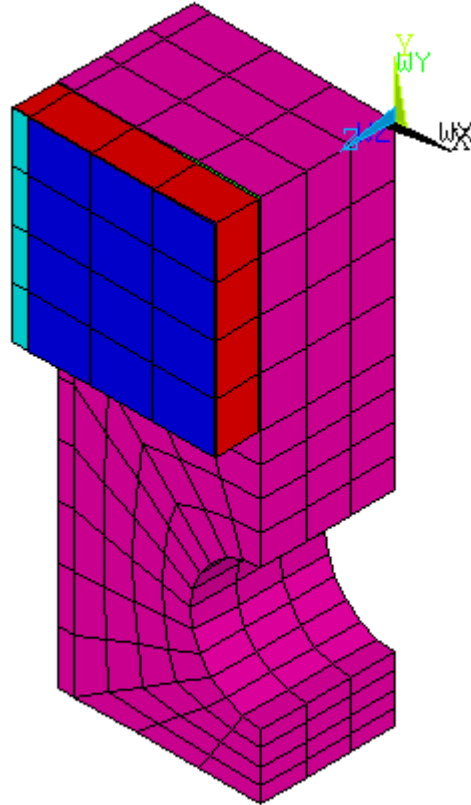
Fig 1.

Two analyses were performed using this model; one using the materials from the "Competition Device", and another using the materials in the "Improved Device". All input stimuli and boundary conditions were the same in both instances.

The applicable material properties from Table 1 were used for these calculations.

Table 1.

Linear Material Properties

Material	Abbr.	Thermal conductivity W/m*K	Thermal Conductivity cal/cm*sec*C	CTE cm/cm/C	CTE in/in/F	Young's Modulus psi	Young's Modulus dyne/cm^2	Source
Aluminum Oxide	Al2O3	39	0.09314994	6.50E-06	3.61E-06			Jack Lackner
Beryllium Oxide	BeO	196	0.46813816	4.70E-06	2.61E-06			Jack Lackner
Copper-Molybdenum-Copper 33-33-33 in plane	Cu-Mo-Cu	311	0.74281106	8.60E-06	4.78E-06			Jack Lackner
Copper-Molybdenum-Copper 33-33-33 perp.	Cu-Mo-Cu	251	0.59950346	8.60E-06	4.78E-06			Jack Lackner
Copper (110)	Cu	397	0.94821862	1.68E-05	9.33E-06			Jack Lackner
Gold Germanium 88-12	AuGe	276	0.65921496	1.28E-05	7.11E-06			Jack Lackner
Lead Indium 50-50	Pb-50 at%In	35	0.0835961	3.06E-05	1.70E-05			Jack Lackner
Thick Film Resistor Metal	????	46	0.10986916	4.70E-06	2.61E-06	5.00E+07	3.44854E+12	Estimate
Platinum Silver	Pt/Ag	73	0.17435758	1.40E-05	7.78E-06			Jack Lackner
Nickel	Ni	89	0.21257294	1.27E-05	7.06E-06			Jack Lackner
Gold	Au	316	0.75475336	1.41E-05	7.83E-06			Jack Lackner
Ceralloy 418	BeO	250	0.597115	9.00E-06	5.00E-06	5.00E+07	3.44854E+12	CenBASE
Ceralloy 418s	BeO	280	0.6687688	9.00E-06	5.00E-06	5.00E+07	3.44854E+12	CenBASE
Copper-Molybdenum-Copper 33-33-33 in plane	Cu-Mo-Cu	311	0.74281106	8.60E-06	4.78E-06	2.70E+07	1.86221E+12	CLIMAX
Copper-Molybdenum-Copper 33-33-33 perp.	Cu-Mo-Cu	251	0.59950346	8.60E-06	4.78E-06	2.70E+07	1.86221E+12	CLIMAX
Gold Germanium 88-12	AuGe	44	0.10509224	1.34E-05	7.42E-06	1.06E+07	7.27643E+11	Indium Corp
Indalloy #7	50 In 50 Pb	22	0.05254612	2.70E-05	1.50E-05	1.94E+06	1.33803E+11	Indium Corp
Indalloy #4	100 In	86	0.20540756	2.48E-05	1.38E-05	1.57E+06	1.08284E+11	Indium Corp

All of the data input to the program was converted to metric units to ensure consistency, as the finite element package used does not validate the units. This means that the stress values shown in the next section are in dyne/cm^2. All temperature values shown are in degrees Celsius.

The stimulus conditions were as follows:

Dissipated Power: 250 Watts C.W.

Heat Sink Temp.: 50 deg. C

Ambient Temp.: 25 deg. C

The ambient temperature is the point from which the thermal induced strains were calculated. Since the material properties used were linear, time invariant quantities, this calculation represents the worst case situation in which there is no relief of stress due to creep effects.

Thermal Results

The temperature contour data for the "Competition Design" is shown in Fig. 2. The corresponding data for the "Improved Design" is shown in Fig. 3. It can be seen, as expected, that the maximum temperature occurs in the center of the resistive film. In both cases the maximum temperature is below 100 deg. C, a very reasonable value for this device. The slightly higher temperature observed in the "Improved Design" is due to the lower thermal conductivity of the Cu-Mo-Cu laminate carrier. The significantly improved CTE match between the laminate carrier and the bond layer in the "Improved Design", however, leads to a significant decrease in the stress induced in the bond layer. This will be demonstrated in the following section.
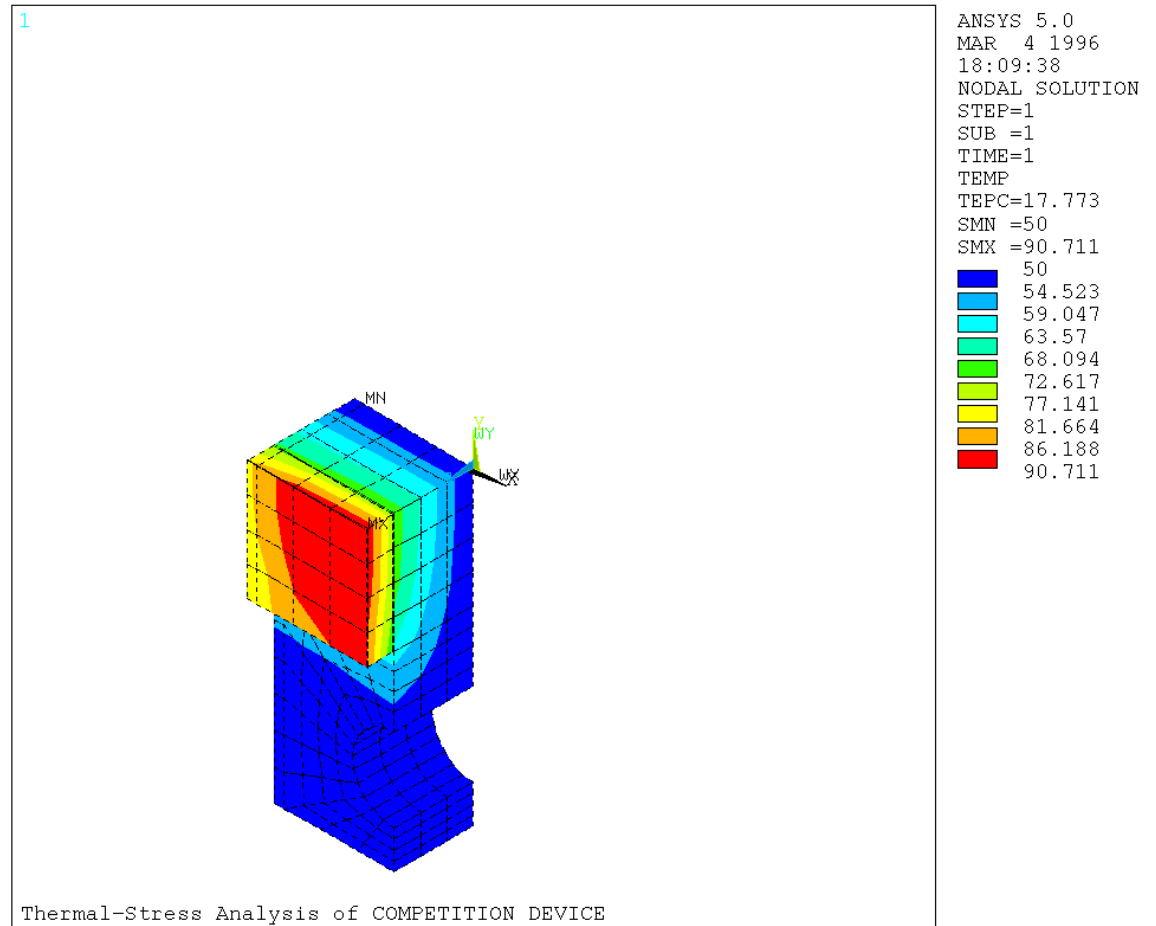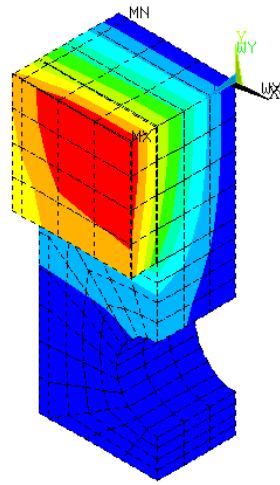

Fig. 2

ANSYS 5.0
MAR 4 1996
18:27:17
NODAL SOLUTION
STEP=1
SUB =1
TIME=1
TEMP
SMN =50
SMX =97.626
```
   50
   55.292
   60.584
   65.875
   71.167
   76.459
   81.751
   87.042
   92.334
   97.626
```

Thermal-Stress Analysis of IMPROVED DESIGN

Fig. 3

Structural Results

The following figures show the calculated stress (von Mises) and strain contours for the bonding layers of both designs. The bonding layer is In-50 / Pb-50 for the "Competition Design". Au-88 / Ge-12 is used in the "Improved Design". Although the strain is reduced by nearly an order of magnitude in the "Improved Design", stress levels are approximately 60~65% compared to those of the "Competition Design". This difference is due to the higher Young's Modulus value for the Gold Germanium material. It should also be noted that the Lead Indium material has a tensile strength of 4670 psi where the Gold Germanium has a tensile strength of 26,875 psi. While tensile strength is not directly related to fatigue effects, it is clear that the "Improved Design" exhibits a significant reduction in both the thermal strain on the bond layer and significant reduction in induced stress.
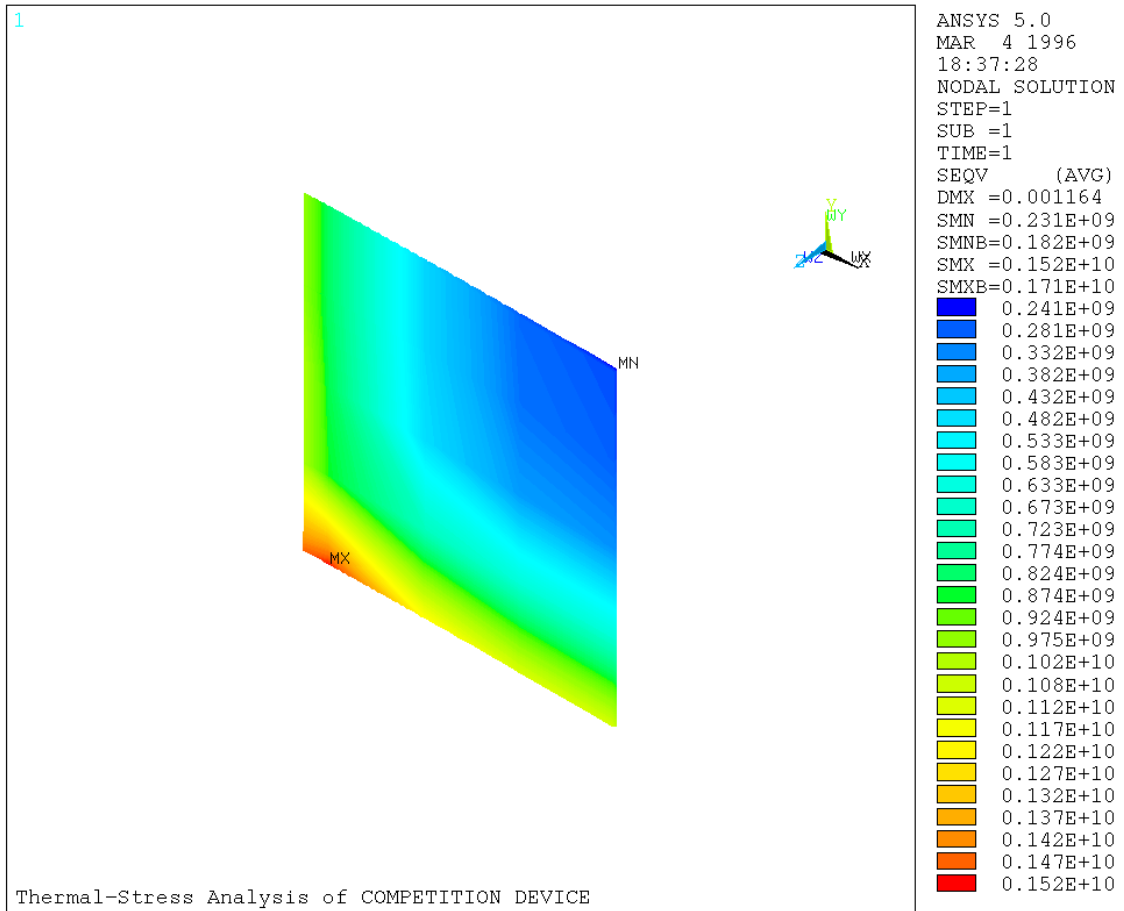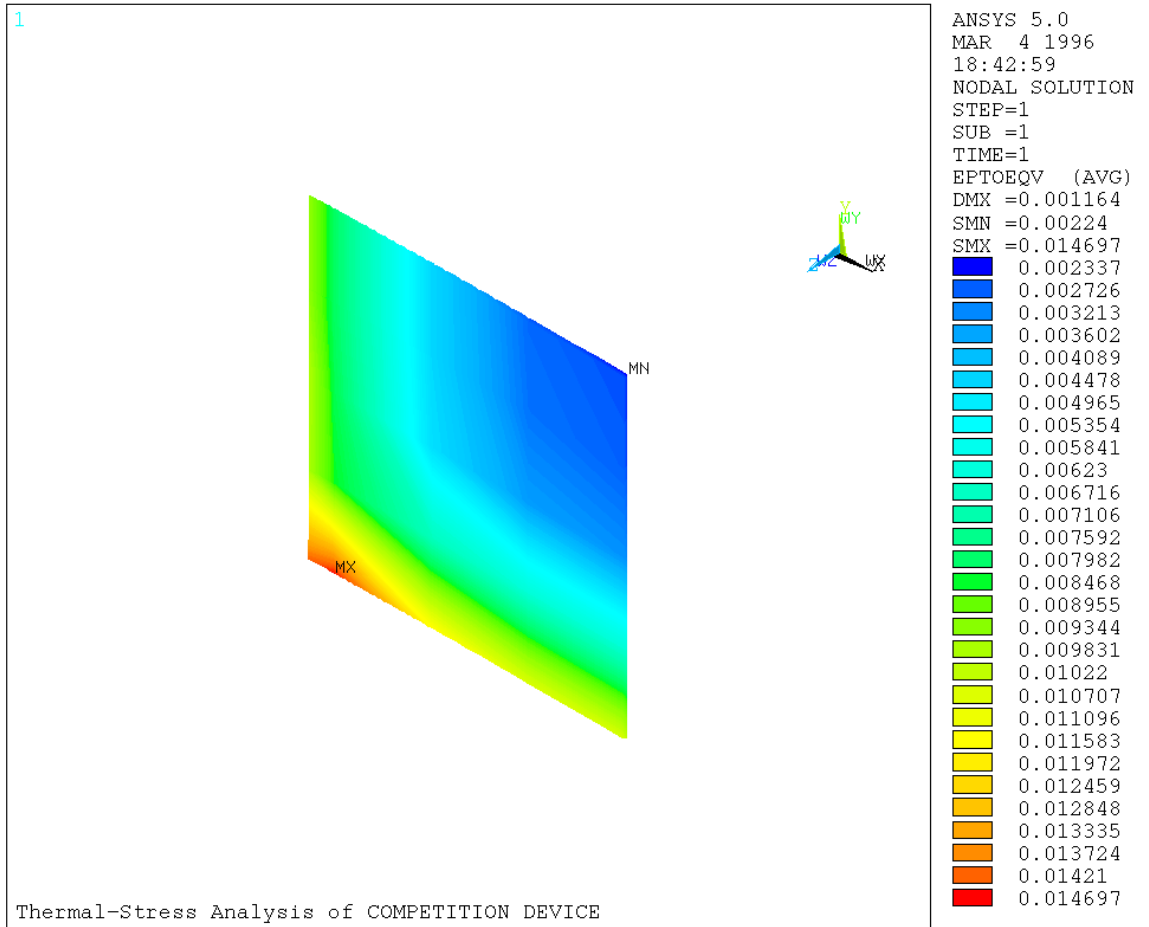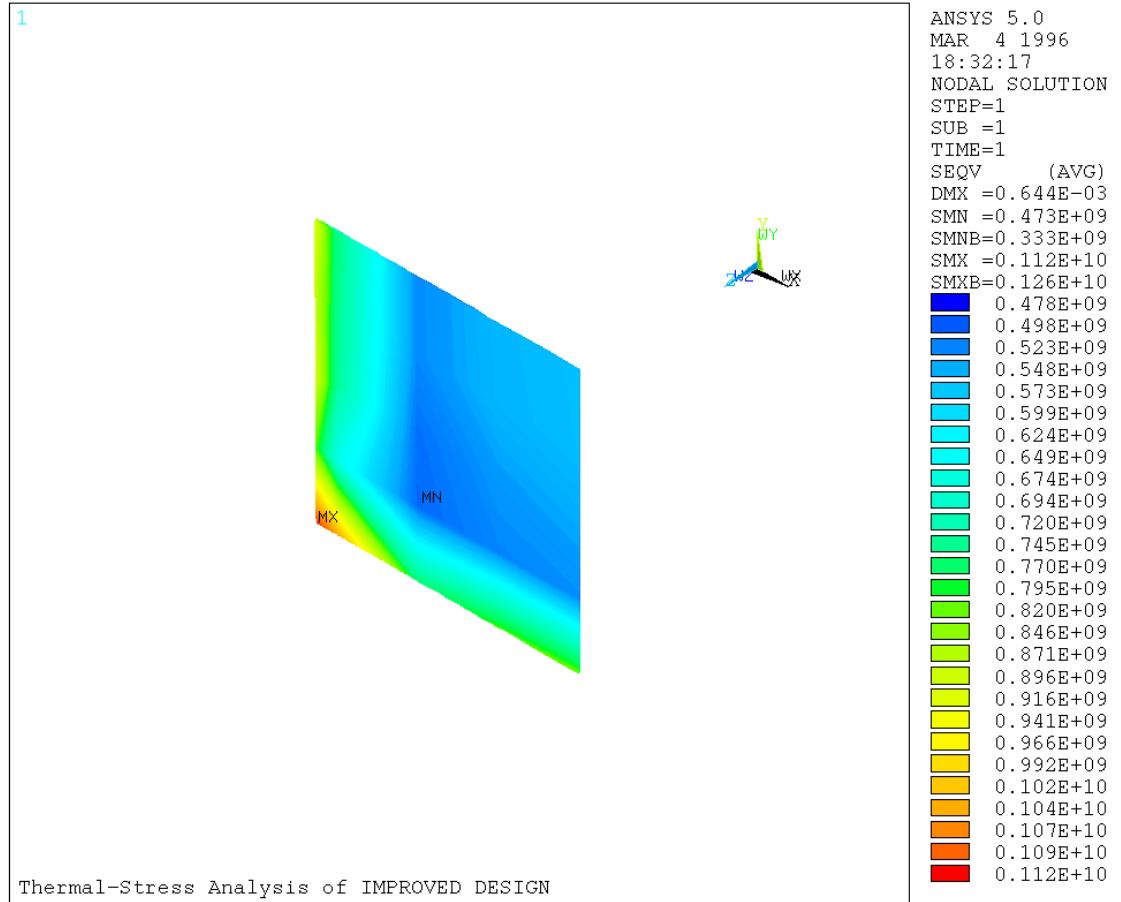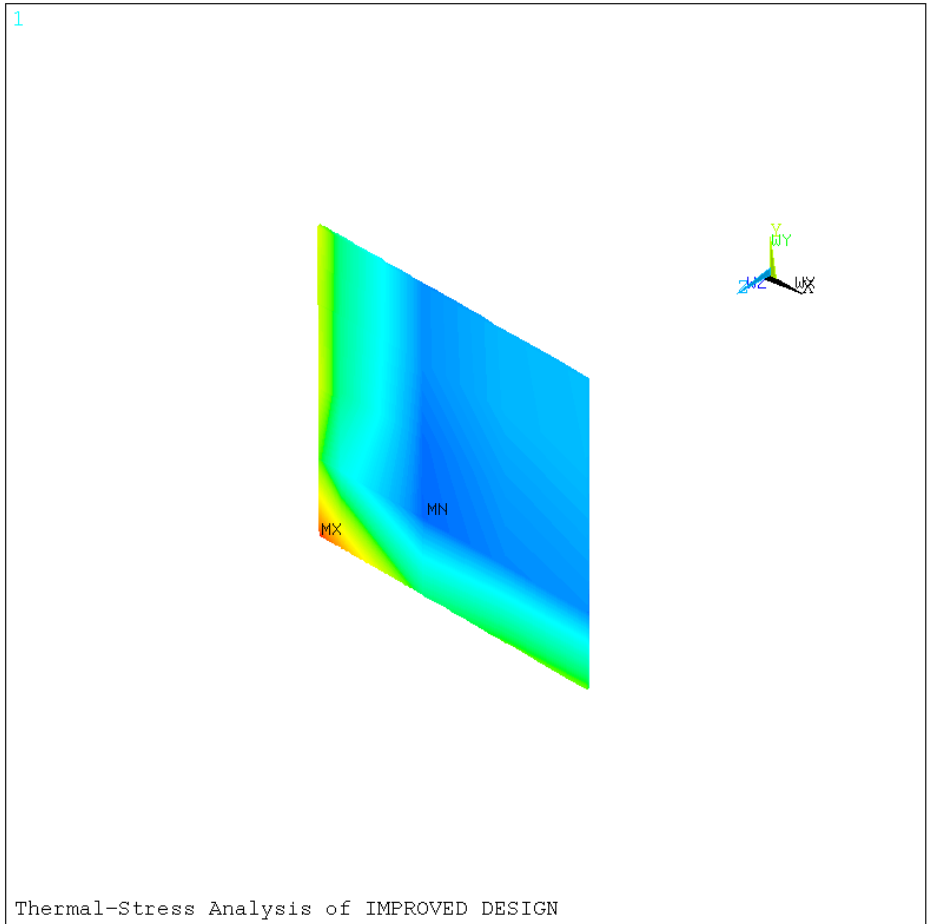

Fig. 4 "Competition Design" Stresses

Fig. 5 " Competition Design" Thermal Strain

Thermal-Stress Analysis of IMPROVED DESIGN

Fig. 6 "Improved Design" Thermal Stresses

ANSYS 5.0
MAR 4 1996
18:44:58
NODAL SOLUTION
STEP=1
SUB =1
TIME=1
EPTOEQV (AVG)
DMX =0.644E-03
SMN =0.845E-03
SMX =0.001997

	0.854E-03
	0.890E-03
	0.935E-03
	0.971E-03
	0.001016
	0.001052
	0.001097
	0.001133
	0.001178
	0.001214
	0.001259
	0.001295
	0.00134
	0.001376
	0.001421
	0.001466
	0.001502
	0.001547
	0.001583
	0.001628
	0.001664
	0.001709
	0.001745
	0.00179
	0.001826
	0.001871
	0.001907
	0.001952
	0.001997

Thermal-Stress Analysis of IMPROVED DESIGN

Fig. 7 "Improved Design" Thermal Strain

Fatigue Analysis

Consideration of fatigue endurance in a cyclic stress condition normally requires examination of several factors relating to the condition of the subject material. The significant factors are:

a)   surface conditions such as scratches, notches, machining marks, etc.

b)   work hardening processes

These factors apply specifically to free surface fatigue. In this case there are effectively no free surfaces, so the conditions in a) above can be ignored. Condition b) above is apparent in the present case and must be included in the analysis.

Work Hardening Effects
The addition of Indium to Lead up to 50% Indium occurs as a continuous series of solid solution alloys. The face centered cubic A1 structure of Lead has a lattice dimension a = 4.9495 angstroms. The addition of Indium, which is tetragonal A6 at 50% Indium, modifies the lattice structure only slightly (a = 4.819 angstroms). The effect of the Indium on the mechanical properties of the alloy is a slight increase in the tensile strength, but no observable change in the elastic limit. There is, however, a significant change in the rate at which work hardening occurs due to the lattice distortion noted above. Since the lattice can no longer readily accommodate the strain (as is possible in the case of pure Lead) microcracking occurs within the matrix and failure by transcrystalline crack propagation occurs with continued applied stress, particularly cyclic stress.

 In the case of the Au/Ge alloy, the solubility of Ge in Gold at temperatures close to ambient is 0.2 atomic % at equilibrium. It has been documented that when used as a brazing alloy, some supersaturation occurs and the Germanium dissolved in Gold is around 1.0 atomic %. This concentration decreases the very high ductility inherent in pure Gold but does not change the capability for stress accommodation.

The tensile strength of the alloy is increased markedly over that of pure Gold, and more significantly, the elastic limit is increased considerably.

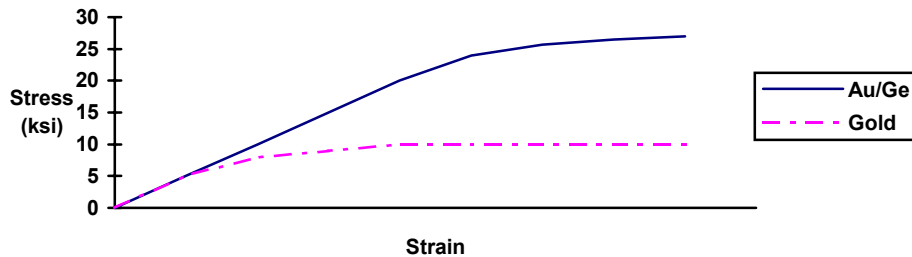The net effects of these considerations are shown in Figure 7 and Figure 8.
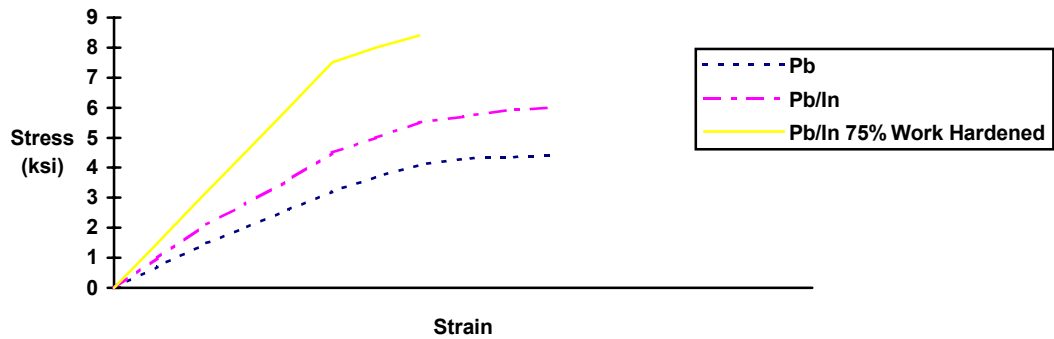

Figure 7

Figure 8

Fatigue Effects

Data empirically derived by Wholer type testing has provided a measure of the relationship between the characteristic elastic limit of metallic elements and alloys and fatigue limit (horizontal sector of δ log N curve).

The ratio for various materials are shown in table 2.

	RATIO	ELASTIC LIMIT	APPROX. FATIGUE LIMIT
Low alloy ferrous metals	**0.48**	**36000**	**18000**
High alloy ferrous metals	**0.5**	**120000**	**60000**
Pure ductile metals	**0.6**	**5000-8000**	**3000-5000**
Soft solders	**0.48**	**3000-7000**	**1500-3500**
Hard solders	**0.52**	**10000-30000**	**5200-16000**

Table 2.

It should be noted that:

1) The ratios shown vary in part due to the capability of various materials to accommodate strain within the lattice structure.

2) The data above is based on equivalent stress in both the positive and negative directions.

In the present case the stress is essentially unidirectional and consequently the ratio will be a higher number, as will the fatigue limit. Therefore, the fatigue limit based on the elastic limits for the two alloys under consideration are Au-Ge, 10,000 psi, and Pb-In, 4000 psi.

Fatigue Limit Data

Figure 9 and Figure 10 show the fatigue limit data for Pb-In and Au-Ge respectively. It demonstrates, for example, that at an effective average stress level in the system of 8000 psi the fatigue endurance limit for Pb-In would be in the range of 100,000 to 200,000 cycles. At the same average stress the fatigue endurance limit for Au-Ge would be in excess of 1 million cycles.

Soft solder alloys are only reliable if the stress applied is sufficiently low to provide limited work hardening. This varies dramatically with the different solder alloys, but all have relatively low fatigue endurance limits. Applied stress on the order of 25,000 psi would be required to lower the fatigue endurance limit of Au-Ge to 100,000 to 200,000 cycles.
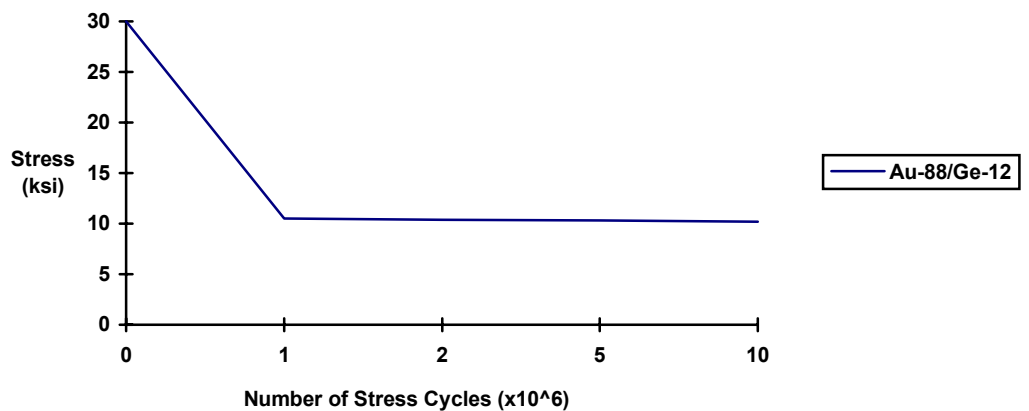

Figure 9

Figure 10

Fatigue Comparison

The peak stress calculated for the "Competition Design" is 22,050 psi. It is clear that since this value is beyond the yield strength of the material, significant plastic deformation occurs within the Pb-In material with each stress cycle.   While this deformation prevents component failure under short cycle (~10^4 cycles) conditions, this design can not be expected to exhibit >10^5 cycle fatigue endurance.

The calculation of peak stress in the "Improved Design" shows a value of 16,240 psi. Although this level is greater than the fatigue limit, the data in Figure 10 indicate that the fatigue endurance limit would be ~650,000 cycles. This represents nearly an order of magnitude improvement over the "Competition Design".

Summary

The results of a thermal - structural analysis of the high power resistors described in the Barry Industries' report "Materials Selection for High-Power / High Reliability Resistors", Jack Lackner, May 1995 have been presented. The conclusions of that report have been supported by quantitative data.